Publ. Astron. Soc. Japan (2016) 68 (3), 43 (1–7)
doi: 10.1093/pasj/psw037
Advance Access Publication Date: 2016 April 22

Mass constraint for a planet in a protoplanetary disk from the gap width

Kazuhiro D. KANAGAWA,[1,2,*] Takayuki MUTO,[3] Hidekazu TANAKA,[1] Takayuki TANIGAWA,[4] Taku TAKEUCHI,[5] Takashi TSUKAGOSHI,[6] and Munetake MOMOSE[6]

[1]Institute of Low Temperature Science, Hokkaido University, Kita-19, Nishi-8, Kita-ku, Sapporo, Hokkaido 060-0819, Japan
[2]Institute of Physics and CASA*, Faculty of Mathematics and Physics, University of Szczecin, Wielkopolska 15, 70-451 Szczecin, Poland
[3]Division of Liberal Arts, Kogakuin University, 1-24-2 Nishi-Shinjuku, Shinjuku-ku, Tokyo 163-8677, Japan
[4]School of Medicine, University of Occupational and Environmental Health, 1-1 Iseigaoka, Yahata-nishi-ku, Kitakyushu, Fukuoka 807-8555, Japan
[5]Department of Earth and Planetary Sciences, Tokyo Institute of Technology, 2-12-1 Ookayama, Meguro-ku, Tokyo 152-8551, Japan
[6]College of Science, Ibaraki University, 2-1-1 Bunkyo, Mito, Ibaraki 310-851, Japan

*E-mail: kazuhiro.kanagawa@usz.edu.pl

Received 2016 January 18; Accepted 2016 March 12

Abstract

A giant planet creates a gap in a protoplanetary disk, which might explain the observed gaps in protoplanetary disks. The width and depth of the gaps depend on the planet mass and disk properties. We have performed two-dimensional hydrodynamic simulations for various planet masses, disk aspect ratios, and viscosities, to obtain an empirical formula for the gap width. The gap width is proportional to the square root of the planet mass, $-3/4$ the power of the disk aspect ratio and $-1/4$ the power of the viscosity. This empirical formula enables us to estimate the mass of a planet embedded in the disk from the width of an observed gap. We have applied the empirical formula for the gap width to the disk around HL Tau, assuming that each gap observed by the Atacama Large Millimeter/submillimeter Array (ALMA) observations is produced by planets, and discussed the planet masses within the gaps. The estimate of planet masses from the gap widths is less affected by the observational resolution and dust filtration than that by the gap depth.

Key words: planet–disk interactions — protoplanetary disks — stars: individual (HL Tau)

1 Introduction

Recent observations of protoplanetary disks have shown disks with non–axisymmetric structures (e.g., Casassus et al. 2013; Fukagawa et al. 2013; van der Marel et al. 2013; Pérez et al. 2014) and/or gap structures (e.g., Osorio et al. 2014; ALMA Partnership 2015). One possible origin of these structures is the dynamic interaction between the disk and embedded planets (Lin & Papaloizou 1979, 1993; Goldreich & Tremaine 1980). A large planet embedded in a disk produces a gap around its orbit. The planet mass

and the disk properties are reflected in the gap width and depth. It is important to construct a model of a gap that can predict a planet's mass.

Recent studies on the gap formation (e.g., Duffell & MacFadyen 2013; Kanagawa et al. 2015a, 2015b, hereafter Paper I) have revealed that the gap depth is related to the planetary mass, the disk aspect ratio (temperature), and the viscosity, as

$$\frac{\Sigma_{\rm min}}{\Sigma_0} = \frac{1}{1+0.04\,K}, \tag{1}$$

where $\Sigma_{\rm min}$ and Σ_0 are the surface densities at the bottom of the gap and at the edge, respectively. The dimensionless parameter K is defined by

$$K \equiv \left(\frac{M_{\rm p}}{M_*}\right)^2 \left(\frac{h_{\rm p}}{R_{\rm p}}\right)^{-5} \alpha^{-1}, \tag{2}$$

where $M_{\rm p}$, M_*, $R_{\rm p}$, $h_{\rm p}$, and α are the masses of the planet and the central star, the orbital radius of the planet, the scale height at $R_{\rm p}$, and the viscous parameter with the prescription by Shakura and Sunyaev (1973), respectively. The gap depth given by equation (1) agrees well with the results of the hydrodynamic simulations (Varnière et al. 2004; Duffell & MacFadyen 2013; Fung et al. 2014).

As seen from equation (1), the gap depth is determined by the dimensionless parameter K, which is a function of $M_{\rm p}$, $h_{\rm p}$, and α. Hence, the planet mass can be estimated from the depth of the observed gap if the disk aspect ratio and the viscosity are given. Paper I applied equation (1) to a gap of the HL Tau disk observed by the ALMA (Atacama Large Millimeter/submillimeter Array) Long Baseline Campaign (ALMA Partnership 2015) and estimated that the lower limit of the mass of the planet within the gap at 30 au is 0.3 $M_{\rm J}$ if this gap originated from the disk–planet interaction. It is, however, very difficult to estimate the mass of a planet in a deep gap because the emission at the bottom of the gap should be measured with a reasonable signal-to-noise ratio. In contrast, the gap width can be more easily measured than the gap depth.

It is known that the width of the gap induced by a planet increases with the planet mass (Takeuchi et al. 1996; Varnière et al. 2004; Duffell & MacFadyen 2013; Duffell 2015; Duffell & Chiang 2015). However, a quantitative relationship between the gap width and the planet mass is not clear. Varniere, Quillen, and Frank (2004) reported that if $(M_{\rm p}/M_*)^2(h_{\rm p}/R_{\rm p})^{-2}\alpha^{-1} \gtrsim 0.3$, the gap edges are between the locations of the $m = 2$ and 1 outer Lindblad resonances. If Keplerian rotation is assumed, the distances between the planet and the $m = 2$ and 1 outer Lindblad resonances are $0.31R_{\rm p}$ and $0.59R_{\rm p}$, respectively (Goldreich & Tremaine 1980). On the other hand, the hydrodynamic simulations performed by Duffell and MacFadyen (2013) show that narrower gaps are created. The half-width of the gap given by Duffell and MacFadyen (2013) is below 0.23 $R_{\rm p}$ even if $(M_{\rm p}/M_*)^2(h_{\rm p}/R_{\rm p})^{-2}\alpha^{-1} > 0.3$ (see figure 6 of their paper). Further investigation has been required in order to constrain the planet mass from the width of the observed gaps.

In this paper, we derive an empirical relationship between the gap width and the planet mass, performing 26 runs of two-dimensional hydrodynamic simulation. In section 2, we describe the numerical method. In section 3, we show our results and the empirical formula for the gap width. We apply the formula to estimate the masses of the planets in the observed gaps of the HL Tau disk in section 4. Section 5 is the summary.

2 Numerical method

We study the shape of the gap induced by a planet embedded in a protoplanetary disk using the two-dimensional hydrodynamic code FARGO (Masset 2000), which is widely used to study disk–planet interaction (e.g., Crida & Morbidelli 2007; Baruteau et al. 2011; Zhu et al. 2011). The computational domain ranges from $R/R_{\rm p} = 0.4$ to 4.0, with 1024 $\times$ 2048 radial and azimuthal zones. The disk scale height, h, is resolved by 22 (radial) and 16 (azimuthal) zones in the vicinity of the planet. For simplicity, we neglect the gas accretion on to the planet and assume the planet rotates on the fixed orbit with $R = R_{\rm p}$. We adopt a constant kinematic viscosity coefficient ν, which is $\nu = \alpha c_{\rm p} h_{\rm p}$, (Shakura & Sunyaev 1973), where $c_{\rm p}$ is sound speed at $R = R_{\rm p}$. The disk aspect ratio h/R is also set to be a constant throughout the disk. We adopted a smoothing length for the gravitational potential of the planet as $0.6h_{\rm p}$. We have checked that the choice of the smoothing length does not significantly influence the gap width.

We perform 26 runs of the hydrodynamic simulation for various planetary masses (0.1 $M_{\rm J}$–2 $M_{\rm J}$, if $M_* = 1\ M_\odot$), disk aspect ratios (1/30–1/15) and the parameter α of the viscosity (10^{-2}–10^{-4}), which are listed in table 1. In this work, we follow 10^4–10^5 orbits at the planet's location to reach the steady state. In the cases with $\alpha = 10^{-4}$, a very long time, i.e., $\sim 10^5$ planetary orbits, is required to obtain the steady gap width. Such long calculations are necessary because of the slow viscous evolution in the less viscous disk.

Initially, the surface density is constant [$\Sigma(R) = \Sigma_0$] in the whole region. The initial angular velocity is given as $\Omega_{\rm K}\sqrt{1-\eta}$, where $\Omega_{\rm K}$ is the Keplerian angular velocity and $\eta = (1/2)(h/R)^2 d\ln P/d\ln R$. The radial drift velocity is given by $v_R = -3\nu/(2R)$. The planet mass smoothly builds up from zero to the final value by using the ramp function defined by $\sin^2[\pi t/(64P_{\rm orbit})]$.

Table 1. Our models and gap widths.

M_p/M_*	h_p/R_p	α	K'	Δ_{gap}/R_p	M_p/M_*	h_p/R_p	α	K'	Δ_{gap}/R_p
5×10^{-4}	1/30	1×10^{-2}	0.68	0.36	5×10^{-4}	1/25	1×10^{-3}	3.91	0.61
1×10^{-3}	1/30	1×10^{-2}	2.71	0.51	1×10^{-3}	1/25	1×10^{-3}	15.6	0.79
5×10^{-4}	1/20	1×10^{-2}	0.20	0.27	3×10^{-4}	1/20	1×10^{-3}	0.72	0.39
1×10^{-3}	1/20	1×10^{-2}	0.80	0.42	5×10^{-4}	1/20	1×10^{-3}	2.00	0.50
5×10^{-4}	1/30	4×10^{-3}	1.69	0.46	7×10^{-4}	1/20	1×10^{-3}	3.92	0.58
1×10^{-3}	1/30	4×10^{-3}	6.77	0.65	1×10^{-3}	1/20	1×10^{-3}	8.00	0.69
5×10^{-4}	1/20	4×10^{-3}	0.50	0.36	1×10^{-3}	1/15	1×10^{-3}	3.37	0.56
1×10^{-3}	1/20	4×10^{-3}	2.00	0.51	2×10^{-3}	1/15	1×10^{-3}	13.5	0.71
1×10^{-3}	1/15	4×10^{-3}	0.84	0.44	1×10^{-4}	1/20	6×10^{-4}	0.13	0.24
2×10^{-3}	1/15	4×10^{-3}	3.37	0.59	5×10^{-4}	1/20	6×10^{-4}	3.13	0.55
5×10^{-4}	1/30	1×10^{-3}	6.77	0.67	1×10^{-3}	1/20	6×10^{-4}	12.5	0.76
1×10^{-3}	1/30	1×10^{-3}	27.1	0.83	1×10^{-4}	1/20	1×10^{-4}	0.80	0.38
1×10^{-4}	1/25	1×10^{-3}	0.16	0.24	5×10^{-4}	1/20	1×10^{-4}	20.0	0.92

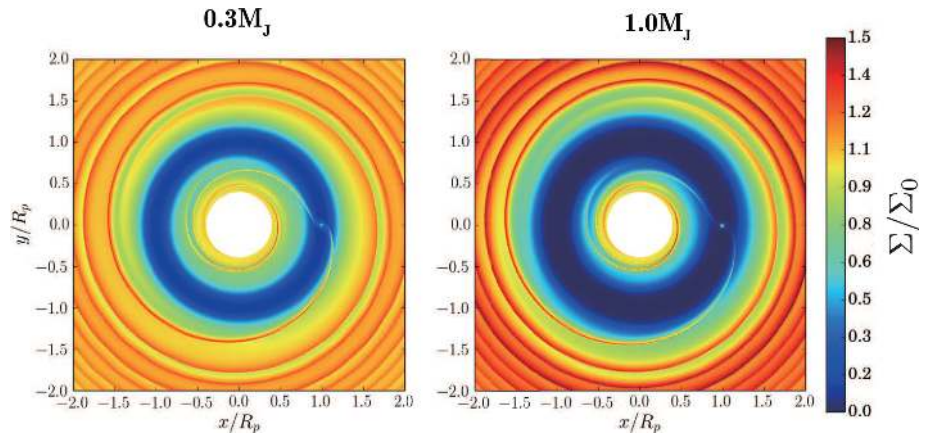

Fig. 1. The surface density distributions at 10^4 planetary orbits obtained by two-dimensional hydrodynamic simulations for $M_p = 0.3\,M_J$ (left) and $M_p = 1.0\,M_J$ (right). Other parameters are set to be $h_p/R_p = 1/20$, $\alpha = 10^{-3}$, and $M_* = 1\,M_\odot$. (Color online)

At the inner and outer boundaries ($R/R_p = 0.4$ and 4.0), we keep the initial condition described above. In addition, we introduce wave-killing zones near the boundaries ($0.4 < R/R_p < 0.5$ and $3.2 < R/R_p < 4.0$) to avoid artificial wave reflection at the boundaries (de Val-Borro et al. 2006).

3 Results

3.1 Empirical formula for the gap width

Figure 1 shows two-dimensional distributions of the surface density at $t = 10^4$ planetary orbits in runs with $M_p = 0.3\,M_J$ and $1.0\,M_J$. To measure the gap width, we take an azimuthal average of the surface density (figure 2). We define the gap region by the radial extent where the azimuthally averaged surface density is smaller than half of the initial surface density. The gap width Δ_{gap} is given by $R_{out} - R_{in}$. Then we obtain radii R_{in}, R_{out} of the inner and outer edges of the gap region. Note that we can make a reasonable guess of the gap width from only the snapshot of the simulations (or observations) since the surface density approaches Σ_0 outside the gap region. The gap width in the case of $1.0\,M_J$ ($\Delta_{gap} = 0.69R_p$) is ~80% larger than that in the case of $0.3\,M_J$ ($\Delta_{gap} = 0.39R_p$).

Figure 3 shows Δ_{gap} against the dimensionless parameter K' defined by

$$K' = \left(\frac{M_p}{M_*}\right)^2 \left(\frac{h_p}{R_p}\right)^{-3} \alpha^{-1}, \tag{3}$$

and they are also recorded in table 1. It is clear that the gap width is well scaled by the parameter K'. We find an empirical formula for the gap width as

$$\frac{\Delta_{gap}}{R_p} = 0.41 \left(\frac{M_p}{M_*}\right)^{1/2} \left(\frac{h_p}{R_p}\right)^{-3/4} \alpha^{-1/4} = 0.41\,K'^{1/4}. \tag{4}$$

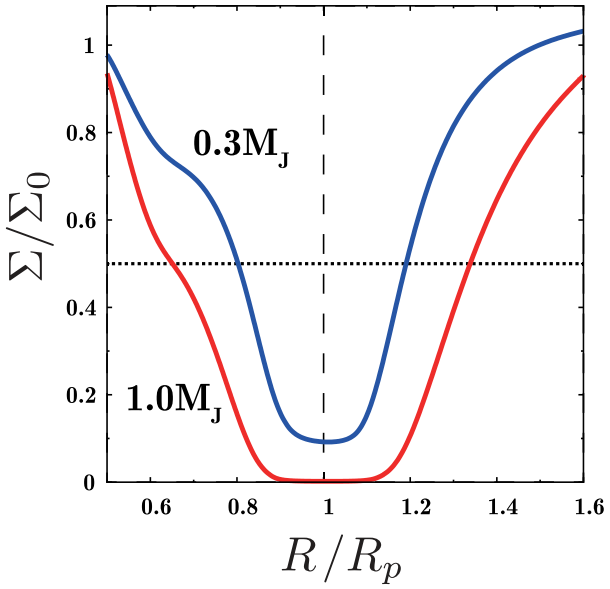

Fig. 2. Radial distributions of the azimuthally averaged surface density for runs with $M_p = 0.3\,M_J$ (blue) and $1.0\,M_J$ (red) presented in figure 1. The horizontal dotted line indicates the level of $\Sigma_0/2$. (Color online)

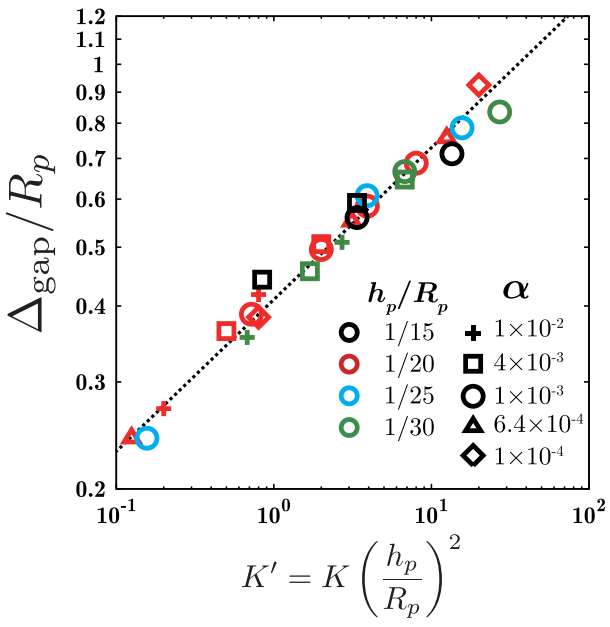

Fig. 3. Widths of the gaps, $\Delta_{gap} = (R_{out} - R_{in})$, against the dimensionless parameter K'. The dotted line is the empirical formula for the gap width given by equation (4). The color of symbols denotes the disk aspect ratio: $h_p/R_p = 1/15$ (black), 1/20 (red), 1/25 (blue), and 1/30 (green). The symbols denote the viscosity: $\alpha = 10^{-2}$ (cross), 4×10^{-3} (square), 10^{-3} (circle), 6.4×10^{-4} (triangle), and 10^{-4} (diamond). (Color online)

As seen from equation (4), the gap width depends weakly on the planet mass and the viscosity, which is consistent with previous studies (Varnière et al. 2004; Duffell & MacFadyen 2013). We also find that the disk aspect ratio affects the gap width as $h_p^{-3/4}$. Solving equation (4) for M_p/M_*, we obtain

$$\frac{M_p}{M_*} = 2.1 \times 10^{-3} \left(\frac{\Delta_{gap}}{R_p}\right)^2 \left(\frac{h_p}{0.05\,R_p}\right)^{3/2} \left(\frac{\alpha}{10^{-3}}\right)^{1/2}. \quad (5)$$

This equation allows us to estimate the planet mass from the observation gap width. The planet mass strongly depends on Δ_{gap} and h_p/R_p, as compared with α. Hence, if Δ_{gap} and h_p/R_p are measured accurately from high-resolution observations, the planet mass can be well constrained. Note that equation (5) should be applied to the gap whose Σ_{min} is smaller than $0.45\Sigma_0$, which is the depth of the most shallow gap in figure 3.

The gap width given by equation (4) is reasonably consistent with that given by the hydrodynamic simulations of Varnière et al. (2004) and Duffell and MacFadyen (2013). Their results have larger scatter, which may be partly due to the short computational time. More detailed discussions on our simulations will be described in a forthcoming paper (K. Kanagawa et al. in preparation).

3.2 Test for the gap formation induced by the planet

The mass of the planet in the gap can be estimated from the gap width [equation (4)] or the depth [equation (1)]. If the width and depth give the same planet mass, it is supported that the gap is formed by a planet. Combining equations (1) and (4), we obtain the relationship between the gap width, the depth, and the disk aspect ratio as

$$\frac{\Delta_{gap}}{R_p} \left(\frac{\Sigma_{min}}{\Sigma_0 - \Sigma_{min}}\right)^{1/4} \left(\frac{h_p}{R_p}\right)^{-1/2} = 0.92. \quad (6)$$

This should be satisfied for a gap created by a planet. Note that equation (6) contains only observable quantities since the aspect ratio can be also estimated by the observed disk temperature. When the gap width and depth are precisely observed in gas emission, equation (6) enables us to judge whether the gap is created by the planet. For the observation of the dust thermal emission, the mass estimate from the gap width [equation (5)] is still useful as long as dust particles are well coupled to the gas, as discussed in the next section.

4 Application to HL Tau disk

Recently, clear axisymmetric gaps in HL Tau disk were discovered in dust thermal emission by the Long Baseline Campaign of ALMA (ALMA Partnership 2015). Recent hydrodynamic simulations can reproduce the observational image of the HL Tau disk using the disk–planet interaction (e.g., Dong et al. 2015; Dipierro et al. 2015;

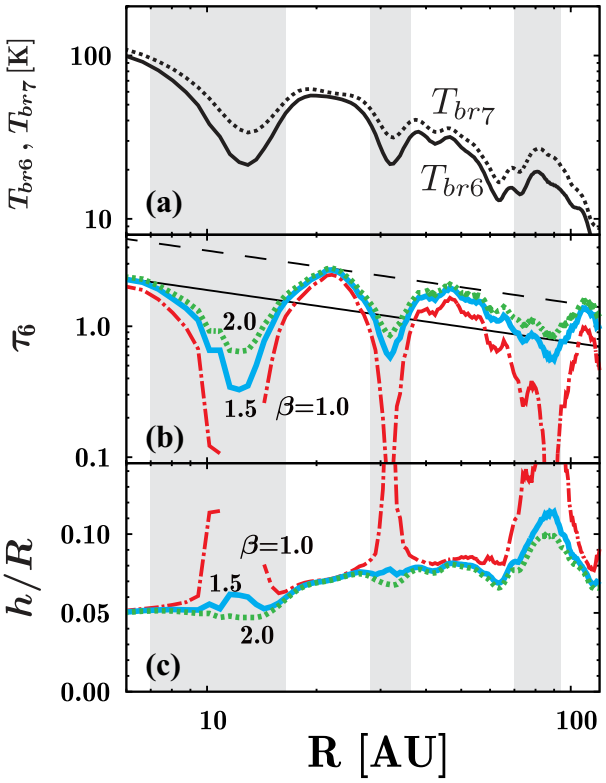

Fig. 4. (a) Observed radial profile of the brightness temperatures of dust continuum emission in the disk of HL Tau along the major axis. The data are averaged over $\pm 15^\circ$ in PA from the major axis (PA $= 138^\circ$ and 318°) after the deprojection of the observed images under the assumption that the inclination angle $= 46.^\circ 7$. The hatched regions indicate the full width for each gap for $\beta = 1.5$. (b) The radial profiles of the optical depth in Band 6. The thin dashed and solid lines denote the unperturbed value of the optical depth $\tau^{\rm unp}$ and $\tau^{\rm unp}/2$ for measuring the gap width (see text). (c) The radial profiles of the aspect ratio obtained by the disk temperature. (Color online)

Picogna & Kley 2015; Jin et al. 2016). In Paper I, we applied equation (1) to estimate the planet mass for the HL Tau disk. In this study, equation (4) is applied to the widths of the observed gap. As done in Paper I, using the brightness temperatures in Bands 6 and 7, we obtain the optical depth in Band 6 and the gas temperature for the assumed spectral index β (figure 4). The disk aspect ratio is calculated from the temperature by $h/R = c/(R\Omega_K)$, where $c = 10^5 (T/300\,{\rm K})^{1/2}\,{\rm cm\,s^{-1}}$. We assume that the mass of the central star is $1\,M_\odot$. We identify three prominent gaps in the optical depth at $R = 10$ au, 30 au and 80 au in figure 4b. Although the gap at 80 au could be regarded as two gaps, Dipierro et al. (2015) pointed out that this structure can be considered as one gap with remaining dust in the horseshoe region. Thus, we assume that the 80-au gap is created by a single planet.

The optical depth outside the gaps can be fitted by $\tau^{\rm unp} = 9.5(R/1\,{\rm au})^{-0.4}$ in figure 4b. We regard $\tau^{\rm unp}$ as the unperturbed surface density to measure the gap width. Note that the opacity is assumed to be constant throughout the disk. The locations of the inner and outer gap edges, $R_{\rm in}$ and $R_{\rm out}$, are determined by intersection points with $\tau^{\rm unp}/2$ and we measure the gap width as $R_{\rm out} - R_{\rm in}$. The location of the planet, $R_{\rm p}$, is simply estimated as $(R_{\rm in} + R_{\rm out})/2$.

Table 2. Measured gap properties and estimated planet masses.*

	$R_{\rm in}$ (au)	$R_{\rm out}$ (au)	$\frac{\Delta_{\rm gap}}{R_{\rm p}}$	$\frac{h_{\rm p}}{R_{\rm p}}$	$M_{\rm p}$ ($M_{\rm J}$) (from the width)
10-au gap	7	16.5	0.81	0.05	1.4
30-au gap	28.5	36	0.23	0.07	0.2
80-au gap	70	94	0.29	0.1	0.5

*We set $\alpha = 10^{-3}$, $\beta = 1.5$, and $M_* = 1\,M_\odot$ at the evaluation in this table.

We assume that the gap widths of the gas and dust disks are similar. That is, it is assumed that dust particles are reasonably coupled to the disk gas and thus the dust filtration is weak. If the dust filtration is strong, the dust surface density is enhanced at the outer edge of the gap by orders of magnitude and is significantly reduced at the inner part of the disk (e.g., Zhu et al. 2012; Dong et al. 2015; Picogna & Kley 2015). In the case of relatively weak filtration, on the other hand, the gap widths of the dust disk are not altered much (see figure 3 of Zhu et al. 2012). Because no significant pile-up of dust is found at the outer edge of each gap in figure 4b, the assumption of the weak dust filtration would be valid for the HL Tau disk. Dong, Zhu, and Whitney (2015) also estimated the mass of the planets in the HL Tau disk by using hydrodynamic simulations that include dust filtration for $\alpha = 10^{-3}$ and $M_{\rm disk} = 0.17\,M_\odot$. Their result indeed shows that the gap width of millimeter-sized dust particles is similar (within a factor of 2) to that of small particles tightly coupled to the gas because of relatively weak dust filtration in the massive disk of HL Tau (see figure 10 of Dong et al. 2015), though the gap depth is much affected even in the case of the weak filtration. Hence the gap width of the dust disk is more suitable for estimating the planet mass than the gap depth of the dust disk. In addition, for particles smaller than millimeter-sized particles, gap widths (and gap depths) in gas and dust are more similar to each other. Jin et al. (2016) have also performed hydrodynamic simulations with 0.15-millimeter-sized particles in similar situation to that of Dong, Zhu, and Whitney (2015) ($\alpha = 10^{-3}$ and $M_{\rm disk} = 0.08\,M_\odot$), and reproduced the observed image of the HL Tau disk. In their simulations, the gap widths in gas and dust are very similar.

Table 2 shows the properties of the observed gaps and the estimated planet masses. In this table, we set $\beta = 1.5$ to obtain the optical depth and the aspect ratio, and adopt $\alpha = 10^{-3}$ for estimating the planet masses. The planet masses for the gaps at 10 au, 30 au, and 80 au are estimated from

the gap widths to be 1.4 M_J, 0.2 M_J, and 0.5 M_J, respectively. The estimated mass of the planet at the 30-au gap is consistent with that estimated from the gap depth in Paper I.

We should note that the gap properties and the estimated masses depend on β, as seen in figure 4b. The radiative transfer model of Pinte et al. (2016) implies that $\beta \simeq 1$. For the innermost gap, the planet mass is estimated to be 3.3 M_J (1.3 M_J) if $\beta = 1$ (2) from the gap width. For the 80-au gap, the gap width is much more affected by the choice of β. The disk aspect ratio can be influenced by the choice of β, which may not be neglected because the planet mass depends relatively strongly on the disk aspect ratio [$M_p \propto (h_p/R_p)^{3/2}$, see equation (5)]. For instance, the disk aspect ratio at the outermost gap can be changed from 0.08 to 0.11 if we vary β from 2.0 to 1.5 (see figure 4c). In this case, the estimated mass of the planet can be changed from 0.35 M_J to 0.57 M_J. Therefore, an accurate estimate of β is essential in deriving the planet mass from the gap shape. Future multi–frequency and high spatial resolution observations may constrain the planet mass better.

The location of the planet (R_p) can affect the mass estimate because the gap width is scaled by R_p in equation (5). Although we simply estimate R_p as $(R_{in} + R_{out})/2$ by assuming a symmetric gap, R_p can be changed because the actual shape of the gap is slightly non–symmetric. Indeed, for instance, R_p for the innermost planet is set to be ~13 au in the previous simulations, which is slightly larger than that in table 2. If $R_p = 13$ au is adopted, the estimated mass of the planet is slightly smaller (1.1 M_J) than that in table 2.

In addition to β and R_p, the planet mass can also depend on the choice of the viscous parameter α, which is highly uncertain. However, the estimate of the planet mass varies only $\alpha^{1/2}$ [see equation (5)] and therefore, the dependency of the planet mass on the viscous parameter is not very strong.

The relatively narrow 10- and 30-au gaps are only marginally resolved with the observation. As seen in figure 2, each gap width measured at the level of $\Sigma_0/2$ is wider than that of the bottom region, which determines the gap depth. For the marginally resolved gap, the gap width can be accurately measured as compared with the minimum surface density of the gap. Hence mass estimated from the gap width is less affected by the resolution.

Dong, Zhu, and Whitney (2015) estimated the planet masses to be 0.2 M_J for these three gaps of the HL Tau disk from their hydrodynamic simulations, by including dust filtration. Their result is consistent with our estimate for the 30-au gap. For the 10-au gap, our estimated mass is much larger than their result. This is probably because quantitative comparison between the model and observations is not the main focus of their work. In their model, the gap width of millimeter-sized dust particles is ~5 au (see their figure 10), which is about half of our measured width for the 10-au gap of the HL Tau disk. If the gap width is halved, the planet mass estimated from the width is four times smaller [see equation (5)]. This partially explains the difference between our results and theirs. We also find a difference of a factor of 2.5 in the planet mass estimate for the 80-au gap. It may be due to the uncertainty in β.

Adopting 0.15-millimeter-sized particles, Jin et al. (2016) have also estimated similar masses of the planets to Dong, Zhu, and Whitney (2015) (0.35 M_J, 0.17 M_J, and 0.26 M_J for the innermost, middle and outermost gaps). Their estimated masses of the planets are smaller than those given by our estimate (table 2), because they assumed the mass of the central star as 0.55 $M_\odot$, which is smaller than that adopted in table 2 (1 $M_\odot$). Adopting $M_* = 0.55\ M_\odot$, we estimate the masses of the planets as 0.77 M_J, 0.11 M_J, and 0.28 M_J for the innermost, middle and outermost gaps, respectively. For the middle and outermost gaps, the estimated planet masses are quite similar to the result of Jin et al. (2016). For the innermost gap, our estimate gives the same mass of the planet as their result if the gap width is narrower by only ~2 au than that measured from figure 4b.

Dipierro et al. (2015) also derived the planet masses from hydrodynamic simulations similar to Dong, Zhu, and Whitney (2015), but by assuming a much less massive disk; $M_{disk} = 0.0002\ M_\odot$. Their result shows a strong filtration at shallow gaps for millimeter-sized particles (figure 3 of Dipierro et al. 2015), in contrast to Dong, Zhu, and Whitney (2015) and Jin et al. (2016). This is reasonable because dust filtration is stronger for a less-massive disk, since the coupling between the gas and dust is weaker. However, the observations suggest that the disk mass should be ~0.1 $M_\odot$ for the HL Tau disk if the gas-to-dust mass ratio is ~100 (Robitaille et al. 2007; ALMA Partnership 2015).

5 Summary

We have derived an empirical formula for the gap width [equation (4)], by performing 26 runs of hydrodynamic simulation. The gap width is expressed as a power-law function of the planet mass, the disk aspect ratio, and the viscosity. This empirical formula enables us to estimate the planet mass from the gap width. Paper I presented the relationship between the gap depth and the planet mass as equation (1). If the gap is created by the planet, the masses estimated by equations (1) and (4) should be consistent, and the gap width and the gap depth should satisfy equation (6). With this, it is possible to check whether the gap is created by a planet when the gap width and depth are accurately observed in the gas emission. For the dust thermal emission, if dust filtration is not very effective, an

estimate of planet mass from the gap width is still useful because the gap widths in the gas and dust disks are not so different.

We have applied the empirical formula for the gap width to the gaps in the HL Tau disk observed in dust thermal emission by ALMA. We have estimated the mass of planets in the gaps at 10 au, 30 au, and 80 au as $1.4\,M_{\rm J}$, $0.2\,M_{\rm J}$, and $0.5\,M_{\rm J}$, respectively, assuming $M_* = 1\,M_\odot$. For the innermost gap, the whole structure may not be completely resolved by the observation and measuring the gap depth is difficult. The dust filtration alters the gap depth more than the gap width. The estimate that results from the gap width gives us a more accurate planet mass than that from the gap depth. Our estimate depends on the particle size of dusts (i.e., the dust opacity index of β) and the disk model for the dust filtration. More sophisticated models in the HL Tau disk would improve the above estimates of the planet mass. If the gap is observed in gas emission, we can constrain a planet mass from the gap depth and width, without uncertainty of the dust and disk models.

Acknowledgement

We thank Ruobing Dong for giving us his data. This paper makes use of the following ALMA data: ADS/JAO.ALMA#2011.0.00015.SV. ALMA is a partnership of ESO (representing its member states), NSF (USA) and NINS (Japan), together with NRC (Canada) and NSC and ASIAA (Taiwan), in cooperation with the Republic of Chile. The Joint ALMA Observatory is operated by ESO, AUI/NRAO and NAOJ. This work was supported by JSPS KAKENHI Grant Numbers 23103004, 26103701, 26800106 and Polish National Science Centre MAESTRO grant DEC- 2012/06/A/ST9/00276. KDK was supported by the ALMA Japan Research Grant of NAOJ Chile Observatory, NAOJ-ALMA-0135. Numerical computations were carried out on Cray XC30 at Center for Computational Astrophysics, National Astronomical Observatory of Japan and the Pan-Okhotsk Information System at the Institute of Low Temperature Science, Hokkaido University.

References

ALMA Partnership 2015, ApJ, 808, L3
Baruteau, C., Meru, F., & Paardekooper, S.-J. 2011, MNRAS, 416, 1971
Casassus, S., et al. 2013, Nature, 493, 191
Crida, A., & Morbidelli, A. 2007, MNRAS, 377, 1324
de Val-Borro, M., et al. 2006, MNRAS, 370, 529
Dipierro, G., et al. 2015, MNRAS, 453, L73
Dong, R., Zhu, Z., & Whitney, B. 2015, ApJ, 809, 93
Duffell, P. C. 2015, ApJ, 807, L11
Duffell, P. C., & Chiang, E. 2015, ApJ, 812, 94
Duffell, P. C., & MacFadyen, A. I. 2013, ApJ, 769, 41
Fukagawa, M., et al. 2013, PASJ, 65, L14
Fung, J., Shi, J.-M., & Chiang, E. 2014, ApJ, 782, 88
Goldreich, P., & Tremaine, S. 1980, ApJ, 241, 425
Jin, S., Li, S., Isella, A., Li, H., & Ji, J. 2016, ApJ, 818, 76
Kanagawa, K. D., Muto, T., Tanaka, H., Tanigawa, T., Takeuchi, T., Tsukagoshi, T., & Momose, M. 2015a, ApJ, 806, L15 (Paper I)
Kanagawa, K. D., Tanaka, H., Muto, T., Tanigawa, T., & Takeuchi, T. 2015b, MNRAS, 448, 994
Lin, D. N. C., & Papaloizou, J. 1979, MNRAS, 186, 799
Lin, D. N. C., & Papaloizou, J. C. B. 1993, in Protostars and Planets III, ed. E. H. Levy & J. I. Lunine (Tucson, AZ: University of Arizona Press), 749
Masset, F. 2000, A&AS, 141, 165
Osorio, M., et al. 2014, ApJ, 791, L36
Pérez, L. M., Isella, A., Carpenter, J. M., & Chandler, C. J. 2014, ApJ, 783, L13
Picogna, G., & Kley, W. 2015, A&A, 584, A110
Pinte, C., Dent, W. R. F., Ménard, F., Hales, A., Hill, T., Cortes, P., & de Gregorio-Monsalvo, I. 2016, ApJ, 816, 25
Robitaille, T. P., Whitney, B. A., Indebetouw, R., & Wood, K. 2007, ApJS, 169, 328
Shakura, N. I., & Sunyaev, R. A. 1973, A&A, 24, 337
Takeuchi, T., Miyama, S. M., & Lin, D. N. C. 1996, ApJ, 460, 832
van der Marel, N., et al. 2013, Science, 340, 1199
Varnière, P., Quillen, A. C., & Frank, A. 2004, ApJ, 612, 1152
Zhu, Z., Nelson, R. P., Dong, R., Espaillat, C., & Hartmann, L. 2012, ApJ, 755, 6
Zhu, Z., Nelson, R. P., Hartmann, L., Espaillat, C., & Calvet, N. 2011, ApJ, 729, 47